Available online at www.sciencedirect.com
SCIENCE DIRECT®
Journal of Nuclear Materials 346 (2005) 226–232
journal of nuclear materials
www.elsevier.com/locate/jnucmat

A model for the effect of the progression of irradiation-induced recrystallization from initiation to completion on swelling of UO_2 and U–10Mo nuclear fuels ☆

J. Rest

Argonne National Laboratory, 9700 S. Cass Avenue, Argonne, IL 60439, USA

Received 19 April 2005; accepted 9 June 2005

Abstract

Analytical expressions are derived for the progression of recrystallization from initiation to completion, and for the swelling due to fission-gas. It is demonstrated that these phenomena can be simulated in both UO_2 and in U–xMo with the same theory, albeit with various property differences. Results of the calculations are compared with available data.

1. Introduction

Irradiation-induced recrystallization appears to be a general phenomenon in that it has been observed to occur in a variety of nuclear fuel types [1], e.g. U–xMo, UO_2, and U_3O_8. The recrystallization process results in sub-micron size grains that accelerate fission-gas swelling due to the combination of short diffusion distances, increased grain-boundary area per unit volume, and greater intergranular bubble growth rates as compared to that in the grain interior [2]. Previously, an expression has been derived for the fission density at which irradiation-induced recrystallization is initiated that is athermal and weakly dependent on fission rate [1]. The initiation of recrystallization is to be distinguished from the subsequent progression and eventual consumption of the original fuel grain.

The driving force for recrystallization is the production of interstitial loops due to irradiation. The continued generation of interstitial loops induces an internal stress in the material which leads to strain in the form of lattice displacement. The initiation of recrystallization has been observed to occur predominately along the preexisting grain boundaries [3]. Subsequently, the recrystallization front moves toward the grain center eventually consuming the entire grain. Thus, the volume fraction of recrystallized material is a function of irradiation time as well as the initial grain size. As gas-bubble swelling is higher in the recrystallized material than in the unrecrystallized fuel, the swelling due to fission gas is a function of the recrystallization kinetics.

Analytical solutions to models for the progression of recrystallization, and for fuel swelling due to fission gas as a function of burnup have been developed.

☆ Work supported by US Department of Energy, Office of Arms Control and Nonproliferation, under Contract W-31-109-Eng-38.

E-mail address: jrest@anl.gov

0022-3115/$ - see front matter © 2005 Elsevier B.V. All rights reserved.
doi:10.1016/j.jnucmat.2005.06.012

Calculations are compared to available data for the volume fraction of recrystallized fuel, and fuel swelling in both UO_2 and U–xMo.

2. Review of model for initiation of irradiation-induced recrystallization

The fission density F_d dependent concentration of viable recrystallization nuclei C_{rx} was determined as a function of the dislocation density ρ_d based on the concept of node pinning by irradiation-induced precipitates associated with fission-gas bubbles [1] as

$$C_{rx} = \frac{9(f(v)\rho_d)^{7/2}}{8\pi^6(C_A C_\rho)^7 F_d^{5/2}}\left(\frac{\alpha_p}{\phi\gamma}\right)^2\sqrt{\frac{2\lambda}{3\pi b_v B_0 \beta}}, \tag{1}$$

where $\phi\gamma/\alpha_p$ is a factor composed of terms related to the production of precipitates and sub-grain growth in the presence of precipitates, b_v is the van der Waals constant, λ is the atom knock-on distance, $f(v) = (1 - v/2)/(1 - v)$, v is Poisson's ratio, C_A is 3 for cubic cells, and C_ρ is within a factor of unity, β is the number of gas atoms produced per fission, and where, at the relatively low temperatures where irradiation-induced recrystallization occurs, the gas atom diffusivity is athermal and can be expressed as $D_g = D_0\dot{f}$, where D_0 is a constant of proportionality and $\dot{f}$ is the fission rate. The temperature dependence of C_{rx} in Eq. (1) is contained in the interstitial and vacancy diffusivities. In general, these diffusivities are expressed as $D_i = D_i^0\exp(-\varepsilon_i/kT)$ and $D_v = D_v^0\exp(-\varepsilon_v/kT)$, where ε_i and ε_v are the interstitial and vacancy migration enthalpies, respectively.

The trigger point for irradiation-induced recrystallization is defined as the point where the kinetically derived concentration of nuclei given by Eq. (1) becomes equal to the equilibrium number of nuclei n_i^* determined from thermodynamic considerations, i.e.

$$n_i^* = n_i^0\exp(-\Delta G^*/kT), \tag{2}$$

where ΔG^* is the critical standard free energy that a node must acquire in order to recrystallize and, as the basic unit out of which the cellular dislocation network is composed is the interstitial loop, n_i^0 is taken to be the athermal component in the expression for the interstitial loop density

$$n_i^0 = \left(\frac{\rho_l}{\pi d_l}\right)_{\text{Athermal}} = \frac{\rho^{3/2}}{\pi^{3/2}C_A C_\rho\sqrt{f(v)}}\exp[+(\varepsilon_v/2 - \varepsilon_i)/2kT]. \tag{3}$$

Equating Eqs. (1) and (2), using Eq. (3), and solving for F_d results in an expression for the critical fission density at which recrystallization will occur, F_{dx}

$$F_{dx} = \left(\frac{\alpha_p\rho_d}{\phi\gamma}\right)^{4/5}\left(\frac{2\lambda}{3b_v D_0\beta}\right)^{1/5} \times \frac{f(v)^{6/5}\exp[4(\varepsilon_v/2 - \varepsilon_i)/15kT]}{\pi^{9/5}(C_A C_\rho)^{12/5}}. \tag{4}$$

The fission density at which recrystallization is predicted to initiate as given by Eq. (4) is athermal and very weakly dependent on fission rate. As such, F_{dx} is independent of ε_v and ε_i and depends primarily on the collision related parameters λ, D_g and $\alpha_p/\phi\gamma$.

Substituting nominal values of the parameters [1] in Eq. (4) leads to the simplified expression[1] for $F_{dx}(m^{-3})$:

$$F_{dx} = 4\times10^{24}(\dot{f})^{2/15}, \tag{5a}$$

$$F_{dx} = 6\times10^{24}(\dot{f})^{2/15}, \tag{5b}$$

where Eq. (5a) corresponds to UO_2 and Eq. (5b) to U–10Mo.

3. Theory for the progression of irradiation-induced recrystallization

A model for the progression of recrystallization as a function of burnup has been developed based on the following assumptions: (1) recrystallization initiates at pre-existing grain boundaries; (2) annuli of width δ, located initially adjacent to the original grain boundary, transform to defect free regions via the creation of the new recrystallized surface when the volumetric strain energy exceeds that necessary to create the new surface; and, (3) the rate at which the defect front moves through the newly created defect free annulus is proportional to the strain rate, which, in analogy with fission-induced creep, is proportional to stress and fission rate. The microscopic stress is a function of the lattice displacement, which is related to the generation rate of interstitial loops.

The original grain boundaries act as nucleation sites for the recrystallization transformation. Upon the initiation of recrystallization, given by Eq. (5), and the creation of the defect-free annulus adjacent to the ring of newly recrystallized material, the defects interior to the annulus are considered to be in a 'superheated' condition. These defects must travel through the denuded annulus in order to find appropriate nucleation sites required for the recrystallization transformation. The defects in the region interior to the defect-free annulus consist of a cellular dislocation network.

When dislocation loops are large enough relative to the inter-atomic distances but small relative to the

[1] Eqs. (3)–(5) are the corrected versions of Eqs. (32)–(34) in Ref. [1].

crystal dimensions, they produce a measurable lattice distortion that can be expressed as

$$\Delta a(t)/a_0 = \pi b_v n_l(t) d_l^2(t)/12. \tag{6}$$

The increase in the lattice parameter is the driving force for irradiation-induced recrystallization. Recrystallization occurs when the strain energy density ΔU in an annulus of width δ is greater than energy required to create new surface, i.e.

$$4\pi r^2 \delta \Delta U = 4\pi r^2 \gamma_{gb}, \tag{7}$$

where γ_{gb} is the energy of the sub-grain boundary and

$$\Delta U = \frac{1}{2}\left(\frac{\Delta a}{a_0}\right)^2 E, \tag{8}$$

where E is the bulk modulus of the material. Thus,

$$\delta = \frac{2\gamma_s \theta}{E(\Delta a/a_0)^2}, \tag{9}$$

where γ_s is the surface energy and θ is the boundary dihedral angle which is given by

$$\theta = 2\mathrm{Tan}^{-1}[b_v\sqrt{\rho_d/2}] \approx 2b_v\sqrt{\rho_d/2}. \tag{10}$$

The progression of recrystallization is assumed to occur in the following sequence of events: (1) subsequent to the formation of the new surface the annulus is cleared of defects; (2) the defect front interior to the annulus is driven through the cleared annulus by stress generated by defect-induced lattice displacement; (3) the strain rate is proportional to stress and fission rate (analogous to fission-induced radiation creep).

The time for the recrystallization front to move a distance $d_g/2 - r(t)$ from the surface of a spherical grain of diameter d_g is given by

$$t_r = \frac{[d_g/2 - r(t)]}{v_{df}}, \tag{11}$$

where v_{df} is the speed of the defect front through the annulus. The volume fraction of recrystallized fuel as a function of time can be expressed as

$$V_r = 1 - \left(\frac{2r(t)}{d_g}\right)^3 \tag{12}$$

and using Eq. (11)

$$V_r = 1 - \left[1 - \frac{2v_{df}t}{d_g}\right]^3. \tag{13}$$

It is here assumed that v_{df} is proportional to the strain rate, i.e.

$$v_{df} = \delta\dot{\varepsilon}, \tag{14}$$

where the strain rate is given by

$$\dot{\varepsilon} = B_2 \dot{f}\sigma \tag{15}$$

and the stress is a function of the lattice displacement

$$\sigma = E\frac{\Delta a}{a_0}. \tag{16}$$

The progression of recrystallization occurs after the cellular dislocation network has formed. Thus, from Eq. (6)

$$\Delta a/a_0 = \frac{b_v C_A C_\rho}{12}\sqrt{\frac{\pi}{f(v)}}\rho_d^{1/2}, \tag{17}$$

where

$$\rho_d = \pi n_l d_l \tag{18}$$

and the lowest energy configuration is a cellular dislocation network with cell size given by [4,5].

$$d_l = C_A C_\rho \sqrt{\frac{\pi}{\rho_d f(v)}}. \tag{19}$$

Using Eqs. (14) and (15) and solving for v_{df}

$$v_{df} = \delta\dot{\varepsilon} = \delta B_2 \dot{f}\sigma. \tag{20}$$

Using Eqs. (9) and (16),

$$v_{df} = \frac{2\gamma_s\theta}{E(\Delta a/a_0)^2} B_2 E\frac{\Delta a}{a_0}\dot{f} = \frac{2\gamma_s 2b_v\sqrt{\rho_d/2}}{(\Delta a/a_0)} B_2\dot{f} \tag{21}$$

and using Eq. (17)

$$v_{df} = \frac{2\gamma_s 2b_v\sqrt{\rho_d/2}}{\frac{b_v C_A C_\rho}{12}\sqrt{\frac{\pi}{f(v)}}\rho_d^{1/2}} B_2\dot{f} = \frac{48\gamma_s B_2}{C_A C_\rho}\sqrt{\frac{f(v)}{2\pi}}\dot{f}. \tag{22}$$

The volume fraction of recrystallized fuel as a function of fission density is then given by

$$V_r = 1 - \left[1 - \frac{2v_{df}t}{d_g}\right]^3, \tag{23}$$

or after substituting Eq. (22) for v_{df}

$$V_r = 1 - \left[1 - \frac{96\gamma_s B_2(F_d - F_{dx})}{d_g C_A C_\rho}\sqrt{\frac{f(v)}{2\pi}}\right]^3. \tag{24}$$

Eq. (24) is the major result of this section. An approximate solution for V_r is given by

$$V_r \approx \frac{288\gamma_s B_2(F_d - F_{dx})}{d_g C_A C_\rho}\sqrt{\frac{f(v)}{2\pi}}, \quad F_d \ll F_d^{max} \tag{25}$$

where

$$F_d = \dot{f}t: \quad F_{dx} = \dot{f}t_x \tag{26}$$

and t_x is the time at which recrystallization is initiated.

Thus, from Eq. (25), for $F_d \ll F^{max}$ the volume fraction of recrystallized fuel is proportional to the fission density and inversely proportional to the grain size. In addition, $V_r(t)$ is independent of fuel temperature.

An estimate of the parameter B_2 is required in order to perform quantitative calculations. U–10Mo fuel with initiation of recrystallization at ~40% burnup appears to reach completion by ~70% burnup. Consistency with

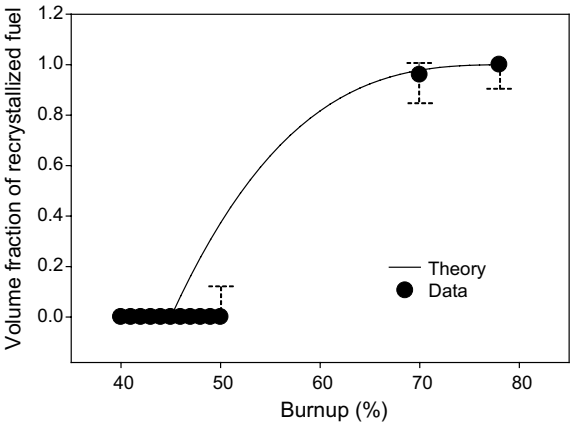

Fig. 1. Volume fraction of recrystallized fuel in U–10Mo calculated with Eq. (24) using $B_2 = 2 \times 10^{-29}$ cm^5/dyne compared with estimated data.

these 'rough' observations requires $B_2 \sim 10^{-29}$ cm^5/dyne. Estimates of this microscopic parameter based on macroscopic in-pile creep data of UO_2 [6] yield $B_2 = 10^{-31}$ cm^5/dyne (i.e. using Eq. (15) with

$\dot{\varepsilon}(UO_2) = 2.8 \times 10^{-10}$ s^{-1},

$\sigma = 2.4 \times 10^8$ dynes/cm^2 and

$\dot{f} = 1.2 \times 10^{13}$ cm^{-3} s^{-1}).

Fig. 1 shows the volume fraction of recrystallized fuel in U–10Mo calculated with Eq. (24) as a function of burnup compared with the estimated data. The calculation shown in Fig. 1 utilized $B_2 = 2 \times 10^{-29}$ cm^5/dyne. Eq. (5b) was used to calculate the initiation of recrystallization at 45% burnup shown in Fig. 1. Although the data shown in Fig. 1 allow an estimate of the value of the parameter B_2, the data are not sufficient to validate the burnup dependence exhibited by Eq. (24). Fig. 2 shows the calculated grain-size dependence of the volume fraction of recrystallized fuel in UO_2 fuel calculated with Eq. (24) compared with data [7]. The grain-size dependence of Eq. (24), i.e. $\approx 1/d_g$ as shown by the approximation given in Eq. (25), is consistent with the trend of the data.

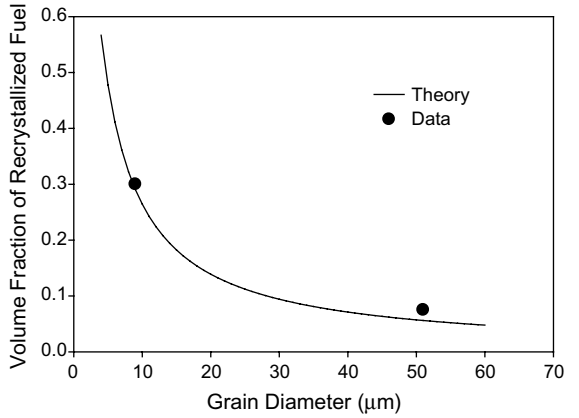

Fig. 2. Calculated grain-size dependence of the volume fraction of recrystallized fuel in UO_2 fuel calculated with Eq. (24) compared with data [7].

4. Effect of recrystallization on fuel swelling

Prior to the onset of recrystallization, the fractional swelling due the accumulated fission gas is given by [8]

$$\left(\frac{\Delta V}{V}\right)_g = \frac{3c_g a^3}{4} + \frac{4\pi}{3}\left(r_b^3 c_b + \frac{3R_b^3 C_b}{d_g}\right), \tag{27}$$

where $\{c_b, r_b\}$ and $\{C_b, R_b\}$ are the intra and intergranular fission-gas bubble density and radius, respectively, and are given by

$$c_b = \frac{16\pi f_n r_g D_0 c_g^2}{b_0 n_b(t)}, \tag{28}$$

$$r_b(t) = \left(\frac{3h_s b_v n_b(t)}{4\pi}\right)^{1/3}, \tag{29}$$

$$C_b = \left(\frac{8zaK}{\pi^2 \xi D_g \delta_{gb}}\right)^{1/2}, \tag{30}$$

$$R_b = \left[\frac{3h_s b_v N_b}{8\pi} + \sqrt{\left(\frac{3h_s b_v N_b}{8\pi}\right)^2 - \left(\frac{N_b kT}{8\pi\gamma}\right)^3}\right]^{1/3} + \left[\frac{3h_s b_v N_b}{8\pi} - \sqrt{\left(\frac{3h_s b_v N_b}{8\pi}\right)^2 - \left(\frac{N_b kT}{8\pi\gamma}\right)^3}\right]^{1/3}, \tag{31}$$

where a^3 is the atomic volume, z is the number of sites explored per gas-atom jump, δ_{gb} is the width of the boundary, ξ is a grain-boundary diffusion enhancement factor, and K is gas-atom generation rate per unit area of grain boundary. Eq. (30) is based on the hypothesis that grain boundary bubble nuclei of radius R_b are produced until such time that a gas atom is more likely to be captured by an existing nucleus than to meet another gas atom and form a new nucleus [9].

The flux K of atoms to the grain boundary in Eq. (30), is given by

$$K = \frac{d_g}{3}\frac{\beta\dot{f} - c_g \mathrm{d}f_s/\mathrm{d}t}{(1 + f_s + 32\pi f_n r_g D_g c_g/b)}\frac{\mathrm{d}(f_s t)}{\mathrm{d}t}. \tag{32}$$

In Eq. (29), the number of gas atoms in an intragranular bubble n_b is given by

$$n_b(t) = \left(\frac{3h_s b_v}{4\pi}\right)^{1/2}\left(\frac{4\pi D_0 c_g(t)}{b_0}\right)^{3/2}, \tag{33}$$

where using conservation of gas atoms, the concentration of gas atoms in solution is

$$c_g(t) = \frac{-(1+f_s) + [(1+f_s)^2 + 64\pi f_n r_g D_g \dot{f} \beta t/b]^{1/2}}{32\pi f_n r_g D_g/b} \tag{34}$$

and the fractional gas release to the boundary

$$f_s = \frac{8}{d_g}\left(\frac{D_g t}{\pi}\right)^{1/2} - \frac{6}{d_g^2} D_g t; \quad 4\pi^2 D_g t/d_g^2 \leqslant 1, \tag{35}$$

$$f_s = 1 - \frac{d_g^2}{60 D_g t} + \frac{3d_g^2}{2D_g t}\exp\left(-\frac{4\pi^2 D_g t}{d_g^2}\right); \quad 4\pi^2 D_g t/d_g^2 > 1. \tag{36}$$

Finally, the number of gas atoms in an intergranular bubble is

$$N_b(t) = \frac{C_g(t)}{C_b(t)}, \tag{37}$$

where

$$C_g(t) = \frac{d_g}{3} f_s(t) c_g(t). \tag{38}$$

In the above equations, β is the number of gas atoms produced per fission event, f_n is the bubble nucleation factor, r_g is the gas-atom radius, $b = b_0\dot{f}$ is the gas-atom re-solution rate, γ is the surface tension, k is Boltzmann's constant, T is the absolute temperature, and h_s is a fitting parameter that for a given T makes the van der Waals equation of state equivalent to the hard-sphere equation of state.

Once recrystallization has been initiated, i.e. using Eq. (5), fuel swelling consists of two components,

$$\left(\frac{\Delta V}{V}\right)_T = (1 - V_r)\left(\frac{\Delta V}{V}\right)_g + V_r\left(\frac{\Delta V}{V}\right)_{gx}, \tag{39}$$

where $(\frac{\Delta V}{V})_g$ is given by Eq. (27), V_r by Eq. (24), and $(\frac{\Delta V}{V})_{gx}$ is given by

$$\left(\frac{\Delta V}{V}\right)_{gx} = 4\pi R_{bx}^3\left(\frac{C_b}{d_g} + \frac{C_{bx}}{d_{gx}} + \frac{1}{3d_{gx}^3}\right). \tag{40}$$

In Eq. (40) it has been assumed that upon recrystallization the preexisting density of bubbles on the boundaries C_b remains relatively unchanged. A new population of bubbles C_{bx} is formed and is given by Eq. (30) with the as fabricated grain size d_g replaced with the recrystallized grain size d_{gx}. The term $1/d_{gx}^3$ represents the density of triple points per unit volume. The triple point nodes are considered very efficient sinks and as such it is assumed that a gas bubble will form at each node. It has also been assumed in Eq. (40) that the radius R_{bx} of the preexisting grain boundary bubbles, the newly formed bubbles and the triple point bubbles are approximately the same.

R_{bx} is given by Eq. (31) with N_b replaced by N_{bx} where

$$N_{bx} = \frac{V_r \beta \dot{f} t}{3\left(\frac{C_b}{d_g} + \frac{C_{bx}}{d_{gx}} + \frac{1}{3d_{gx}^3}\right)}. \tag{41}$$

In Eq. (41), it has been assumed that in the recrystallized region of the fuel the majority of the generated gas is on

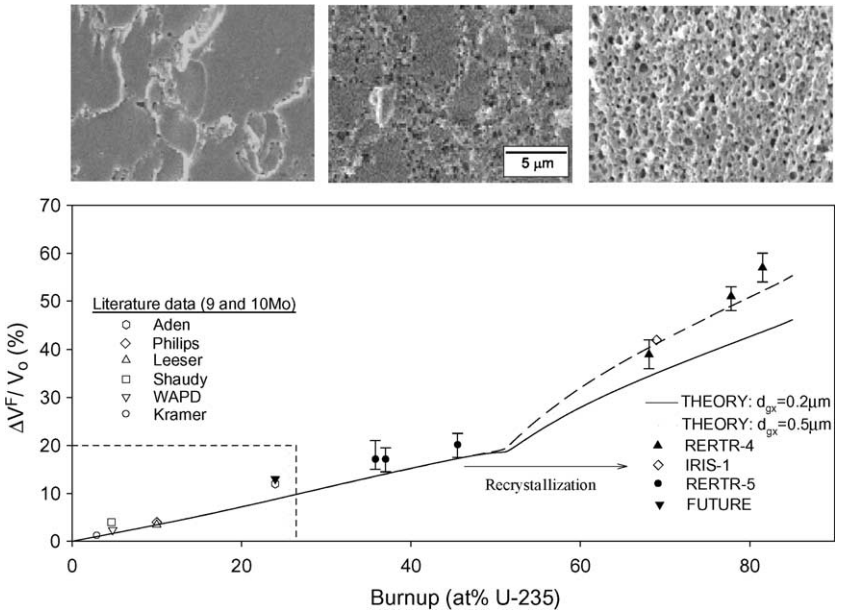

Fig. 3. U–xMo fuel swelling behavior vs. burnup compared with theory for two values of the recrystallized grain size. The measured recrystallized grain size is ≈0.2–0.5 μm.

the grain boundaries. This assumption is consistent with the fractional gas release calculated using Eq. (36) for $4\pi^2 D_g t/d_g^2 > 1$.

Fig. 3 shows data for U–xMo total fuel swelling behavior vs. burnup [10] compared to the theory (i.e. Eqs. (39), (24), (27) and (40)) for two values of the nominal recrystallized grain size. Various parameters used in the calculations are listed in Table 1. The nominal recrystallized grain size d_{gx} represents the average grain size of the distribution of recrystallized grain sizes [11]. A calculation of d_{gx} is the subject of a paper currently in process by this author (submitted to J. Nucl. Mater., July 2005). A solid fission product swelling contribution has been added to Eq. (39) that is given by [12]

$$\left(\frac{\Delta V}{V}\right)_S = 0.014\mathrm{BU}, \tag{42}$$

where BU is the percent burnup with respect to all the metal atoms.

Table 1
Values of various parameters used in the calculations

Parameter	Value	References
β	0.25	[13]
ξ	1.65×10^{3}	[8]
b_0	10^{-23} m^3	[14]
D_0	1.2×10^{-39} m^5	[15]
r_g	0.216 nm	[13]
γ	1 J m^{-2}	[13]
b_v	8.5×10^{-29} m^3/atom	[13]
f_n	10^{-2}	[8]
h_s	0.6	[8]
B_2	2×10^{-34} m^{5}N^{-1} (U–xMo) 10^{-34} m^{5}N^{-1} (UO$_2$)	This work
δ_{gb}	2×10^{-9} m	[8]
z	4	[8]

From Fig. 3 it is clear that the theory follows the trends of the swelling data as a function of burnup across the transition from no recrystallization to full recrystallization. The three micrographs located above the graph in Fig. 3 show, respectively, the fuel prior to recrystallization, at the initiation of recrystallization, and when approximately 100% of the fuel volume has been recrystallized. As seen in the second micrograph of Fig. 3, the initiation of recrystallization occurs primarily along the original grain boundaries. The recrystallized grain size measured from the micrographs in Fig. 3 is ≈0.2–0.5 μm.

Fig. 4 shows U–xMo fuel swelling behavior vs. burnup for two values of the as-fabricated grain size. The effect of the progression of recrystallization, shown in Fig. 4, is a marked suppression in the swelling (solid line as compared to the dashed line in Fig. 4) subsequent to the initiation of this irradiation-induced transformation. From Fig. 4 it is also clear that the effect of the progression of recrystallization (as compared to simultaneous recrystallization of the whole grain) is greater the larger the as-fabricated grain size.

Fig. 5 shows UO_2 fuel swelling behavior based on measured relative immersion density [8] vs. burnup compared with theory ($d_{gx} = 0.2$ μm) for two values of the microscopic strain-rate parameter. The dotted lines in Fig. 5 indicate the spread in measured density values. A solid fission swelling rate of 0.32%/10 GWd/tM [1] was added to Eq. (39) in order to calculate the total fuel swelling. It is interesting to note that the UO_2 solid fission product swelling is ≈3 times larger than that used for U–xMo (Eq. (42)). For burnups greater than 80 GWd/tM, a value of B_2 equal to that used for U–xMo results in UO_2 swelling rates that are larger than those measured. The results shown in Fig. 5 suggest that the value of B_2 in UO_2 is about a factor of 2 smaller than was used for the U–xMo alloy (e.g. see Fig. 3).

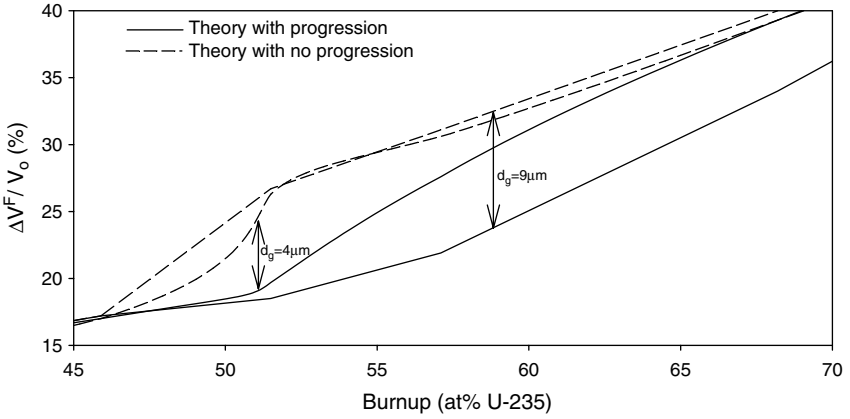

Fig. 4. U–xMo fuel swelling behavior vs. burnup with and without the effects of the progression of recrystallization ($d_{gx} = 0.4$ μm) for two values of the as-fabricated grain size.

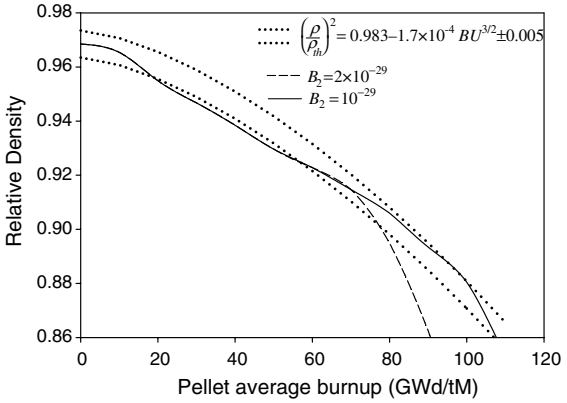

Fig. 5. UO_2 fuel swelling behavior based on measured relative immersion density [8] vs. burnup compared with theory ($d_g = 7$ μm; $d_{gx} = 0.2$ μm) for two values of the microscopic strain-rate parameter.

5. Conclusions

The irradiation-induced swelling behavior of UO_2 and U–xMo has attributes that are remarkably similar. The onset of recrystallization, the progression of recrystallization, and gas-bubble swelling can be simulated in both fuels with the same theory, albeit with various property differences such as fission-induced microscopic creep (e.g. the parameter B_2 in Eq. (15)). That the defect behavior in these two quite dissimilar materials is similar may be ascribed to the dominant role played by the U-atom interstitial loop in each material, and by the athermal character of fission-gas behavior for the irradiation conditions where irradiation-induced recrystallization is operative.

References

[1] J. Rest, J. Nucl. Mater. 326 (2004) 175.
[2] J. Rest, J. Nucl. Mater. 321 (2003) 305.
[3] J. Rest, G.L. Hofman, in: Proceedings of the Materials Research Society Meeting, Symposium R, Boston, MA, November 2000.
[4] J. Rest, G.L. Hofman, J. Nucl. Mater. 277 (2000) 231.
[5] N. Hanson, D. Kuhlmann-Wilsdorf, Mater. Sci. Eng. 81 (1986) 141.
[6] D.R. Olander, Fundamental Aspects of Nuclear Reactor Fuel Elements, Energy Research and Development Administration, TID-26711-P1, 1976, p. 361.
[7] K. Nogita, K. Une, M. Hirai, K. Ito, Y. Shirai, J. Nucl. Mater. 248 (1997) 196.
[8] J. Spino, J. Rest, W. Goll, T. Walker, J. Nucl. Mater., to be published.
[9] M.H. Wood, K.L. Kear, J. Nucl. Mater. 118 (1983) 320.
[10] G.L. Hofman, M.R. Finlay, Y.S. Kim, Post-Irradiation Analysis of low enriched U–Mo/Al dispersion fuel miniplate tests, RERTR 4&5, in: Proceedings of the 2004 RERTR Meeting, Vienna, Austria, 1–5 October 2004.
[11] J. Spino, K. Vennix, M. Coquerelle, J. Nucl. Mater 231 (1996) 179.
[12] Gerard L. Hofman, Leon C. Walters, in: R.W. Cahn, P. Haasen, E.J. Kramer (Eds.), Materials Science and Technology A Comprehensive Treatment, in: Brian R.T. Frost (Ed.), Nucl. Mater., Vol. 10A, Weinheim, New York, 1994, p. 1.
[13] D.R. Olander, Fundamental Aspects of Nuclear Reactor Fuel Elements, Energy Research and Development Administration, TID-26711-P1, 1976.
[14] M.O. Marlow, A.I. Kaznoff, in: Proceedings of the International Conference on Nuclear Fuel Performance, British Nuclear Energy Society, London, 1973.
[15] Hj. Matzke, Radiat. Eff. 53 (1980) 219.